Langmuir

Article

pubs.acs.org/Langmuir

Molecular Simulation Study of the Competitive Adsorption of H_2O and CO_2 in Zeolite 13X

Lennart Joos,[†,‡,∥] Joseph A. Swisher,[†,§,∥] and Berend Smit*[,†,§]

[†]Department of Chemical and Biomolecular Engineering, University of California, Berkeley, California 94720, United States

[‡]Center for Molecular Modeling, Ghent University, Zwijnaarde, B-9052 Belgium

[§]Materials Sciences Division, Lawrence Berkeley National Laboratory, Berkeley, California 94720, United States

Supporting Information

ABSTRACT: The presence of H_2O in postcombustion gas streams is an important technical issue for deploying CO_2-selective adsorbents. Because of its permanent dipole, H_2O can interact strongly with materials where the selectivity for CO_2 is a consequence of its quadrupole interacting with charges in the material. We performed molecular simulations to model the adsorption of pure H_2O and CO_2 as well as H_2O/CO_2 mixtures in 13X, a popular zeolite for CO_2 capture processes that is commercially available. The simulations show that H_2O reduces the capacity of these materials for adsorbing CO_2 by an order of magnitude and that at the partial pressures of H_2O relevant for postcombustion capture, 13X will be essentially saturated with H_2O .

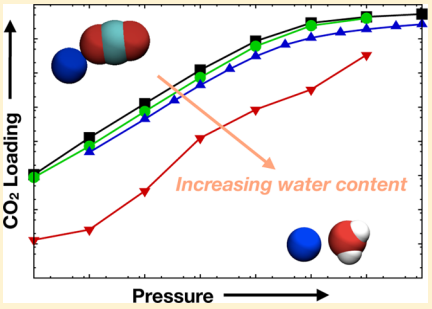

INTRODUCTION

Carbon capture and sequestration has been identified as a critical technology for reducing the impact of fossil fuel use on the concentration of CO_2 in the atmosphere. Although switching to renewable energy sources would eliminate carbon emissions, no technology has been developed that could effectively scale to replace fossil fuels in the near future. Hence, any selection of technologies to reduce carbon emissions in the near term will have to include some form of carbon capture and sequestration.[1−3] The standard industrial method for removing CO_2 from gas streams, known as scrubbing, involves contacting the gas stream with a concentrated solvent containing amines, typically monoethanolamine. However, the energy penalty for this process is high and a variety of alternative processes have been proposed, including membranes, advanced solvents, and adsorption.[4,5]

Zeolite 13X (NaFAU) has been used as a reference material for CO_2 adsorption due to its high selectivity and commercial availability on the tonne scale.[6−8] Zeolites are porous aluminosilicate materials that have been used extensively in industrial adsorption processes, as the small pores and specific topology can sieve molecules based on their kinetic diameter. Moreover, the presence of aluminum gives these frameworks a net negative charge that is compensated by cations in the pore. These cations provide good adsorption sites for the quadrupolar CO_2 molecule, and CO_2/N_2 selectivities up to 300 are found in cation-exchanged zeolite frameworks.[9]

At the same time, these cations might interact strongly with water molecules[9−11] that are present in large quantities in post-combustion gas streams (around 5−15 vol.%).[12] In fact, 13X is marketed as a desiccant in some contexts and has been studied as a medium for storing solar thermal energy with water as the working fluid.[13,14] Understanding the influence of water on CO_2 adsorption is important because it could potentially reduce the capability of materials to selectively adsorb CO_2 efficiently enough for a practical process.

The adsorption of H_2O on aluminosilicate zeolites has been studied by several groups. In an experimental study, Wang and LeVan determined both the pure component and mixture isotherms of H_2O and CO_2 on commercial 13X and 5A samples and noted that small amounts of water reduce the CO_2 capacity slightly. When water is adsorbed near its saturation loading, the CO_2 capacity is an order of magnitude lower than on the dry materials.[15,16] Brandani and Ruthven studied the effect of water on CO_2 and propane adsorption at different water loadings on low-silica forms of X and CaX and correlated the water loading with an exponential decrease in the Henry's law coefficient for CO_2.[17] Finally, experiments by Ferreira et al.[18] and Lee et al.[19] also show that H_2O has a detrimental effect on the CO_2 adsorption capacity of X-type zeolites.

In addition to these experimental studies, there have been a variety of computer simulations performed on water in aluminosilicate zeolites. Castillo et al. compared different H_2O models in pure-silica zeolites and showed that the predicted isotherms were sensitive to the partial charges and crystal structure of the zeolite framework,[20] indicating the need for a well-designed forcefield. This is certainly true when considering water adsorption in frameworks with different Si/Al ratios, as was shown by Di Lella et al.[21] Lee et al. and Faux et al. performed molecular dynamics (MD) simulations of

Received: February 17, 2013
Revised: December 1, 2013
Published: December 6, 2013

water and sodium molecules in zeolite 4A using a fixed and flexible zeolite framework respectively, indicating differences between these two approaches.[22,23] Beauvais et al. simulated water in NaX and NaY (NaFAU at approximately 1.24 and 2.4 Si/Al, respectively) and observed that water can cause a rearrangement of the cations from their preferred sites in the dehydrated structure.[24] These observations are supported by Bellat et al., who demonstrated that there is a small amount of hysteresis at relatively low pressures in NaY, which they attribute to rearrangement of cations between the supercage and sodalite cages of FAU as water adsorbs.[25] Moreover, Boddenburg et al. proposed that some Na cations would be coordinated by up to 6 water molecules near saturation.[26] Finally, Hutson et al. showed that in LiLSX (low-silica X) even a small amount of adsorbed water caused a precipitous drop in the N_2 adsorption capacity that required regeneration above 500 K to recover.[27]

In this computational study, we aim to understand the adsorption of pure H_2O and CO_2 as well as H_2O/CO_2 mixtures in hydrophilic zeolites. Grand Canonical Monte Carlo (GCMC) simulations were used to predict adsorption isotherms and heats of adsorption and Canonical Monte Carlo (CMC) simulations were performed to study the average structure of sodium, H_2O, and CO_2 at different loadings.[28]

METHODS

For our simulations in zeolite 13X, we used the faujasite topology reported by Olson.[29] In the unit cell, aluminum atoms were randomly assigned to 86 T positions (Si/Al ratio of 1.24), respecting Löwenstein's rule, an empirical rule that excludes aluminum atoms in adjacent T-sites. The positions of the framework atoms are kept fixed at all times, since earlier studies showed that this does not have a significant influence on the adsorption of small molecules such as CO_2 and H_2O.[30,31] Sodium atoms were placed randomly as counterions for the aluminum atoms in the framework and were equilibrated using canonical Monte Carlo moves. We allowed the sodium atoms to move during all simulations; for a good idea about the Na distribution in the framework, we refer to work of Beauvais et al. and Bellat et al.[24,25]

Figure 1 shows two views of the 13X framework through the 12-ring connecting the supercages (along the ⟨111⟩ direction). On the left, the atomic structure of the material with the positions of the green extra-framework sodium atoms taken from a Monte Carlo simulation. On the right, a simplified view of the FAU topology, only showing the T-atom positions. The red circle in the center shows the center of one supercage, which is connected to 4 other supercages by 12-rings of T-atoms, the blue circles indicate the sodalite or β-cages of the material. In our simulations, Na and H_2O are allowed to enter both the supercages and sodalite cages, but CO_2 can only access the supercages, not the sodalite cages.

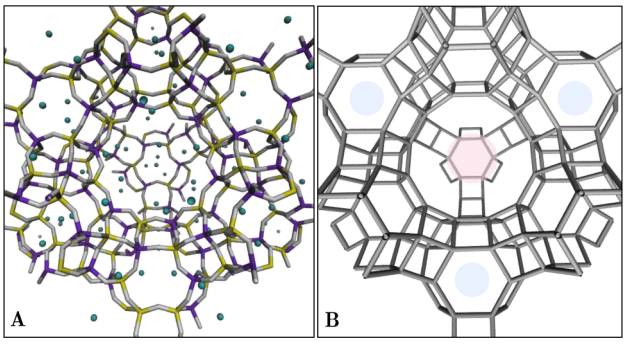

Figure 1. Views of the structure of 13X. (A) A view of the unit cell of 13X (NaFAU), Na positions taken from one configuration of a Monte Carlo simulation. Oxygen atoms are gray, silicon are yellow, aluminum are violet, and sodium are green. (B) Schematic representation of the FAU topology showing the connection between T-atom positions. The blue circles indicate the sodalite cages and the red one the center of the supercage.

Adsorbate molecules were allowed to make either translation, rotation, swap, and regrowth moves. Swap moves involve the insertion or deletion of a single molecule to or from the simulation box. The regrowth move involves taking an existing molecule in the simulation and placing it at another location in the box at random. Interactions between the framework, cations, and adsorbed molecules were modeled using a sum of a 12-6 Lennard-Jones (LJ) term (representing dispersive interactions) and a Coulombic term (including electrostatic interactions). The Ewald summation technique is used to compute the electrostatic contribution.

Lennard-Jones parameters and partial atomic charges for the CO_2-framework, CO_2–Na and CO_2–CO_2 interactions were taken from the force field developed by García-Sánchez et al.[32] and values for σ and ε are printed in the left side of Table 1. H_2O–H_2O interactions were modeled using the SPC/E model.[33] Finally, H_2O-framework and H_2O–Na interactions were parametrized by multiplying the H_2O–H_2O parameters by the ratio of CO_2-framework to CO_2–CO_2 interactions or CO_2–Na to CO_2–CO_2 interactions respectively. In this scaling, it is important to account for the fact that for water there is only an interaction for O_2, while for CO_{H2O}, there are interactions for both C_{CO_2} and O_{CO_2}.

Table 1. Lennard-Jones Parameters Used in This Work[a]

	ε/k_b	σ		ε/k_b	σ
	K	Å		K	Å
C_{CO_2}–C_{CO_2}	29.933	2.745	O_{spce}–O_{spce}	78.197	3.1656
C_{CO_2}–O_{CO_2}	50.640	2.880			
O_{CO_2}–C_{CO_2}	85.617	3.017			
C_{CO_2}–O_{13X}	37.595	3.511	O_{spce}–O_{13X}	85.152	3.723
O_{CO_2}-O_{13X}	78.980	3.237			
C_{CO_2}–Na	362.292	3.320	O_{spce}–Na	564.881	3.361
O_{CO_2}–Na	200.831	2.758			

[a] H_2O-framework and H_2O–Na interactions were parametrized by multiplying the SPC/E H_2O–H_2O parameters by the ratio of CO_2-framework to CO_2 –CO_2 interactions or CO_2–Na to CO_2–CO_2 interactions reported by García-Sánchez et al.[32]

To illustrate our reasoning, we elaborate the determination of $\varepsilon_{O_{13X}-O_{spce}}$ as an example. First, two ratios r_{ε_C} and r_{ε_O} are computed, representing the ratio of CO_2-framework to CO_2–CO_2 interactions for both C and O

$$r_{\varepsilon_O} = \frac{\varepsilon_{O_{13X}-O_{CO_2}}}{\varepsilon_{O_{CO_2}-O_{CO_2}}} \quad (1)$$

$$r_{\varepsilon_C} = \frac{\varepsilon_{O_{13X}-C_{CO_2}}}{\varepsilon_{C_{CO_2}-C_{CO_2}}} \quad (2)$$

The resulting multiplication factor is the average of the r_{ε_C} and r_{ε_O} ratio, so for $\varepsilon_{O_{13X}-O_{spce}}$ this would give

$$\varepsilon_{O_{13X}-O_{spce}} = \frac{1}{2}(r_{\varepsilon_O} + r_{\varepsilon_C})\varepsilon_{O_{spce}-O_{spce}} \quad (3)$$

A similar reasoning was applied for the unknown σ and ε parameters in Table 1. Although the σ parameters for the H_2O -framework and H_2O–Na interactions are relatively large, this force field seems to reproduce the adsorption isotherm for H_2O in 13X very well (see below). However, these parameters may not be transferrable

dx.doi.org/10.1021/la403824g | Langmuir 2013, 29, 15936–15942

to other frameworks or systems and a more detailed analysis of the force field was out of the scope of this work.

Although CO_2 could react with water, we assume that no carbonic acid is formed during adsorption because the force field we used cannot describe this reaction. Moreover, we expect that water interacts more strongly with the Na cations than with CO_2 and that therefore the reaction to HCO_3^- would be slow.

From a practical point of view, it is useful to consider the predicted loadings when a gas stream would be saturated with water. This is the case when the postcombustion gas stream had been subjected to desulfurization processes. Table 2 shows the saturation vapor pressures

Table 2. Saturation Vapor Pressure of Water from the Antoine Equation[34]

T (K)	P_{vap} (kPa)
273	3.14
323	12.25
373	100.78

for water at the temperatures where the isotherm was simulated.[34] Finally, we mention that all loadings are displayed in mol/kg, that is, mol adsorbent per kilogram zeolite, in order to be easily compared with experiments. Note that 1 mol/kg corresponds to 11.434 molecules per unit cell, or that one molecule per unit cell corresponds with 0.088 mol/kg.

RESULTS AND DISCUSSION

In this section, we will first discuss the pure components, CO_2 and H_2O, their isotherms, as well as the adsorption energy as a function of the loading and the arrangement of the adsorbed molecules inside the framework. All information is assembled in Figure 2 in order to provide a clear overview and an easy comparison between CO_2 and H_2O After the analysis of the pure component systems, we will consider CO_2/H_2O mixtures and assess the influence of both components on the isotherm and the adsorbate arrangement.

First of all, Figure 2a shows a good agreement between the water isotherms obtained from our GCMC simulations and experimental data reported in Wang and LeVan.[15] In the Supporting Information, we show that the results also agree well with experimental data from Ferreira et al.[18] and furthermore, we provide the plots on a linear scale. Note that the experiments were conducted on pelletized zeolite samples, but we assume that the influence of the binder is minimal.

Our simulations reveal three distinct regions in the H_2O isotherm. The Henry's law regime is situated at partial pressures well below 1 Pa, that are very difficult to obtain with experiments, as loadings are lower than one water molecule per unit cell. Second, we observe a sharp rise in the loading of water over a narrow pressure range. This behavior can be understood by considering the desorption enthalpy in function of the H_2O loading in Figure 2b. At low loadings, H_2O molecules have high desorption enthalpies (up to 78 kJ/mol), so in this region there is a large thermodynamical driving force for H_2O molecules to adsorb in the framework. This large value then quickly drops as more water molecules are present in the pores, affecting the slope of the adsorption isotherm. Third, there is a plateau region where a significant increase in partial pressure has only a small influence on the water loading. For a postcombustion process around 323 K, the H_2O partial pressure is about 12 kPa (see Table 2), which would place the equilibrium loading within this plateau regime.

Next, we consider CMC simulations that provide insight into the arrangement of the cations and the H_2O molecules at different loadings. We did not use the concept of crystallographic cation positions to analyze and report these arrangements, because this approach assumes that the cations are frozen during the simulations and since we observe big displacements of the cations, the idea is only of limited usefulness.[25,24] Instead, we opted to provide histograms that in our view give similar information more elegantly. Figure 2c shows histograms of the distances between sodium atoms and the oxygen atom in H_2O . The average distance is about 3.5 Å and the peak shifts to slightly smaller distances as the H_2O loading increases. This average distance is larger than the 2.76 Å distance reported for the coordination of sodium cations by water in aqueous solution.[35] The discrepancy between these values will be partly due to the different environment but can also stem from from the relatively large value of σ used for the Na−H_2O interaction in this work (see Table 1).

The interaction between the adsorbing water molecules is illustrated with Figure 2d, where the nearest distances between the oxygen and hydrogen atoms on different water molecules is plotted. The peak at shorter distances (1.7−1.9 Å) represents the interaction of hydrogen bonded molecules, while the peak around 3.2 Å is indicating two water molecules coordinated to the same sodium. As the water loading increases, the density of the latter disappears while the former increases. The stabilization of the water molecules hence shifts from the interaction with the Na cations to the formation of a hydrogen bond network.

Although the adsorption of water is stabilized by the ability to form a hydrogen bond network, water is still interacting strongly with the cations in the zeolite pores. This is clear from Figure 2e, showing the distribution of nearest distances between sodium cations and the aluminum in the framework at different water loadings and 323 K. At low water loading, there is a single peak at short distances, indicating that the sodium cation tends to stay close to the balancing negatively charged aluminum sites. At intermediate water loading, the height of this peak is smaller and there is a longer tail in the distribution because water can stabilize Na further away from the aluminum sites. At the highest water loading, a small second peak appears around 7.4 Å, showing that some of the sodium atoms can be "dissolved" from the surface of the zeolite pore and can be completely coordinated by H_2O in the pore. This is only the case for the sodium cations in the supercages. Water molecules do not enter the sodalite cages (although they were not excluded from it in our calculations) and hence do not alter the positions of the cations that are present there. A similar behavior was observed in a molecular dynamics study on Na-mordenite: water extracts the cations in the main channels and leaves the cations in the smaller channels untouched.[36] Another paper from the same group reports the cation migration in NaX when methanol is absorbed.[37]

The results of the GCMC simulations for the second pure component, CO_2, are presented in the right-hand column of Figure 2, so they can be easily related to those of H_2O. First, in Figure 2f the simulated CO_2 isotherm is compared with the previously mentioned experiments from Wang and LeVan[15] and again shows fair agreement. In the Supporting Information, more experimental isotherms are considered, all of which show good agreement between theory and experiment, both on a log−log scale and on a linear scale.[7,9,18] As opposed to the H_2O isotherm, the CO_2 isotherm does not reveal a steep region at lower fugacities. Moreover, the desorption enthalpy shows virtually no dependence on the loading (Figure 2g). This

dx.doi.org/10.1021/la403824g | Langmuir 2013, 29, 15936−15942

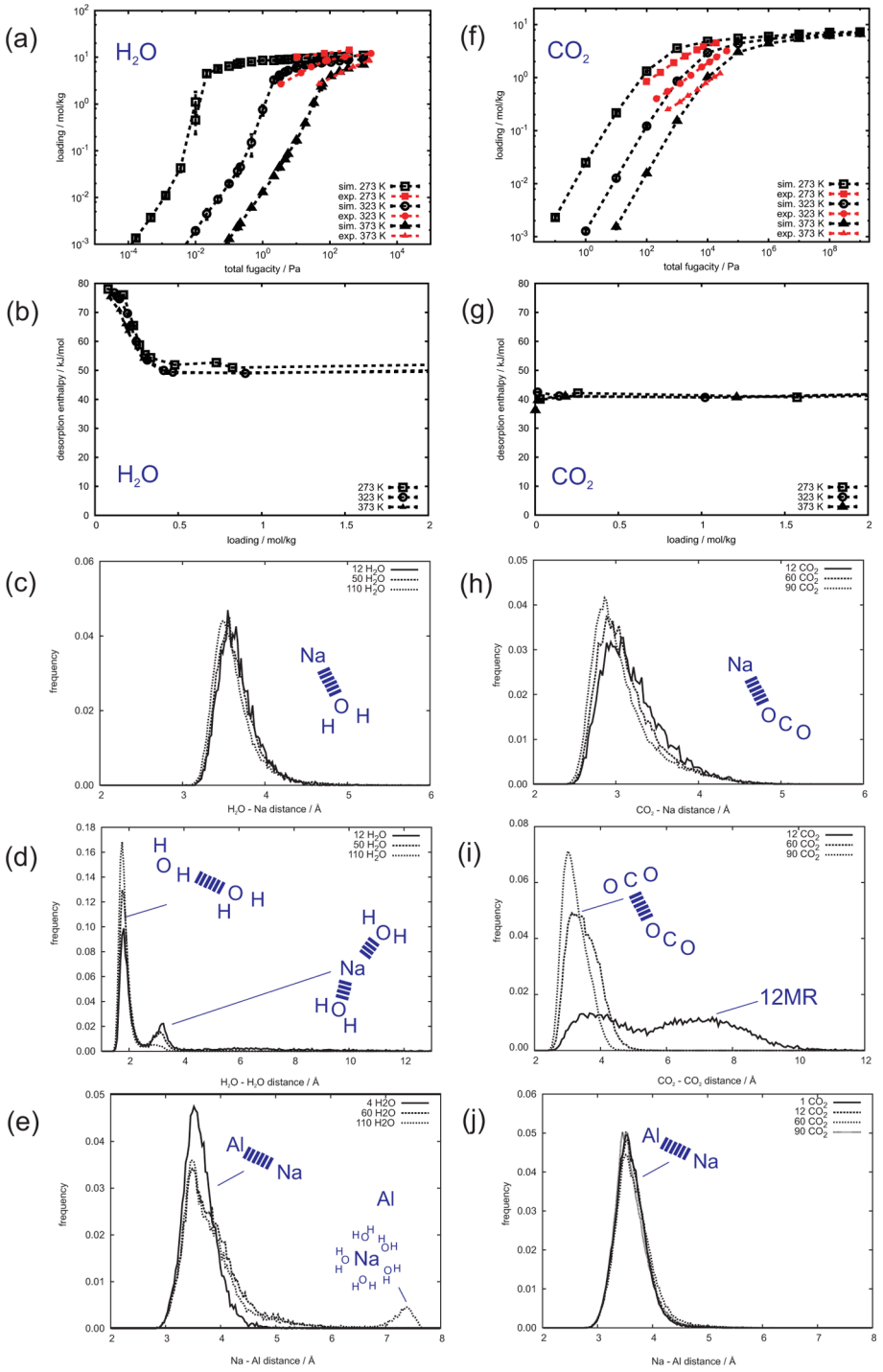

Figure 2. Pure component isotherms with experimental references[15] (a,f), heats of desorption (b,g), and histograms providing an idea about the geometrical configurations (c–e,h–j) for H_2O and CO_2 adsorbing in zeolite 13X.

strengthens our previous conclusion that the shape of the isotherm is related to the evolution of the desorption enthalpies in function of the loading. Note that in typical exhaust gas conditions (325 K and CO_2 partial pressures around 15 kPa, that is, 15% CO_2 at 1 bar) the framework would not be saturated with CO_2, in sharp contrast to water.

CMC simulations at 323 K and at different total loadings of CO_2 provide more information about the average geometry. First, Figure 2h shows histograms of the distribution of Na–O_{CO_2} distances. As the loading of CO_2 increases, the shape of the distribution stays essentially the same, and the peak value shifts to slightly lower distances as the higher density forces the CO_2 molecules together.

Next, Figure 2i presents the distributions of the distance between the O atom in one CO_2 molecule and the C atom in the closest neighboring CO_2 molecule. At low loadings, there are two broad peaks. The first one at distances around 4 Å is associated with CO_2 molecules that are stabilizing each other at a relatively close distance. The second peak between 6 and 8 Å corresponds to the distance between two CO_2 molecules that are sitting in neighboring 12-membered rings, which was

dx.doi.org/10.1021/la403824g | Langmuir 2013, 29, 15936–15942

identified as the preferred adsorption site for CO_2 at low loadings in our simulations. As the loading increases, the CO_2 molecules will be forced together and the interaction between CO_2 molecules becomes more important, resulting in only one peak that is shifted to lower distances.

Finally, Figure 2j shows that the histograms of the distances between sodium and aluminum atoms in the framework in the presence of different loadings of CO_2 remains essentially the same. Compared to H_2O, CO_2 does not influence the positions of sodium atoms, indicating a weaker interactions between CO_2 and sodium. Although Plant et al. report in a theoretical study[38] that CO_2 can cause the migration of a sodium cation, no such effect was observed in our simulations.

As an intermediary conclusion, it is clear from the pure component simulations that H_2O has a much stronger interaction with zeolite 13X than CO_2: 13X is more easily saturated with H_2O, the desorption enthalpies are significantly higher, and the H_2O molecules have an influence on the position of the sodium cations.

Mixture adsorption isotherms were simulated to quantify the influence of water in the adsorption of H_2O/CO_2 mixtures. Figure 3 shows the H_2O and CO_2 isotherms for a 1% H_2O in

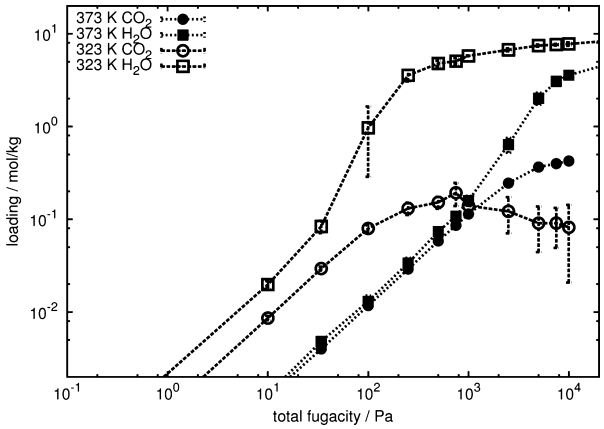

Figure 3. Mixture isotherms for a 99% CO_2, 1% H_2O mixture adsorbing in zeolite 13X at 323 and 373 K.

CO_2 mixture at 323 and 373 K. At low pressures, the two components appear to adsorb independently, which is not surprising as the loadings in this regime are as low as 0.1 mol/kg, or less than 1 molecule per unit cell. The inflection point in the H_2O isotherm is around 100 Pa at 323 K and 3400 Pa at 373 K, corresponding to water partial fugacities of about 1 and 34 Pa, respectively. Once the water isotherms pass the inflection point and enter the plateau regime, the corresponding CO_2 isotherms pass through a maximum and begin to decrease even as the total fugacity continues to increase. Overall, water adsorbs close to its pure component loading, while the capacity for CO_2 adsorption falls drastically.

To improve sampling of the CO_2 isotherms, we performed simulations where CO_2 was treated with GCMC moves and H_2O was treated with CMC moves. Figure 4 shows the adsorption isotherms for CO_2 at different total water loadings at 323 K. As expected, increasing the water loading reduces the equilibrium loading of CO_2 at all pressures. When 13X is near saturation loading (108 or 110 H_2O molecules per unit cell), the CO_2 uptake is more than an order of magnitude lower than for the pure CO_2 component. In the Supporting Information, the isotherms from Figure 4 are compared with experimental

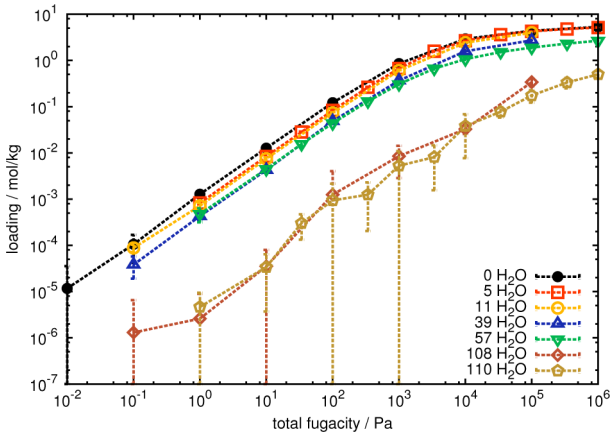

Figure 4. Adsorption isotherms for CO_2 in 13X with fixed loadings of water at 323 K. Water loadings are reported in molecules per unit cell. As the concentration of water in the material increases, the equilibrium CO_2 loading is reduced due to the occupation of pore volume and competition for coordination sites at the sodium cations.

isotherms measured by Wang et al.[39] There is a fair agreement at low water loadings, but a large discrepancy for the isotherm at 108 H_2O molecules per unit cell, which we were not able to explain.

To more effectively study the structure of the adsorbed solution of CO_2 and H_2O, NVT simulations were performed at different numbers of CO_2 and H_2O molecules. Figure 5 shows

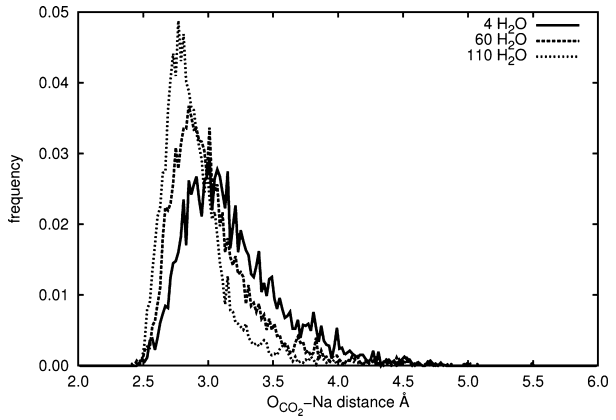

Figure 5. Histograms of O_{CO_2}–Na distances with different constant loadings of H_2O and 8 CO_2 per unit cell at 323 K.

the distribution of Na–O_{CO_2} distances at different H_2O loadings. The CO_2 loading was fixed at 8 molecules per unit cell. As with pure CO_2, the average distance between Na and the oxygen atom in CO_2 decreases. At the highest water loading, the most likely distance is smaller than for the pure CO_2 case (2.8 Å vs 3 Å). As the water hydrogen bonding network becomes more extensive, it is more favorable to force the CO_2 molecule closer to the Na cations than to disrupt the network. Next, Figure 6 shows the distribution of O–H distances between different water molecules as the water loading increases with 8 CO_2 molecules per unit cell. The previously mentioned trend that it becomes more likely to find the H_2O molecules within hydrogen bond distance as the loading increases, does not seem to be disrupted by the presence of CO_2 molecules. The formation of a hydrogen bond

dx.doi.org/10.1021/la403824g | Langmuir 2013, 29, 15936–15942

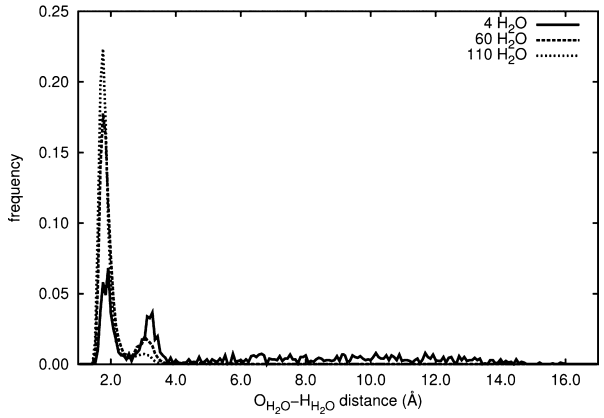

Figure 6. H_2O–H_2O distance histograms at different loadings of H_2O and 8 CO_2 per unit cell at 323 K.

network will also tend to exclude CO_2 since a CO_2 molecule is easily replaced by another water molecule.

In this study, we only considered the isotherms of CO_2 and H_2O, but a typical flue gas contains around 80% of N_2. Although we don't expect a significant influence, this is certainly worth a thorough investigation. Moreover, it would be interesting to investigate the influence of the Si/Al ratio of the framework, for instance, by considering low silica X or zeolite Y.

■ CONCLUSIONS

We have performed a molecular simulation study of H_2O and CO_2 adsorption in zeolite 13X, a prototypical alumniosilicate zeolite that is commercially available. Our model is able to reproduce the trends in experimental isotherms for H_2O and CO_2 at different temperatures. Moreover, we were able to ascribe the steep rise in the H_2O isotherm to the relatively high desorption enthalpy at low loadings. Generally, H_2O tends to form an extensive hydrogen bond network and is even able to dislodge sodium cations from the zeolite framework surface and stabilize it in the center of the pore. CO_2 on the other hand does not have a large influence on the sodium cations but is also shows good structuring near saturation loading.

When a mixture of H_2O and CO_2 adsorbs, H_2O dominates and adsorbs near its pure component isotherm, which dramatically reduces the available adsorption sites for CO_2 . At flue gas conditions, with a CO_2 and H_2O partial pressures of about 15 and 12 kPa respectively, water will likely be adsorbed near its saturation loading, and the CO_2 loading will be reduced by an order of magnitude.

In conclusion, this behavior dramatically reduces the utility of these materials for postcombustion capture and expensive drying operations may be required to allow 13X to provide sufficient CO_2 adsorption capacity.

■ ASSOCIATED CONTENT

Supporting Information

Additional information and figures. This material is available free of charge via the Internet at http://pubs.acs.org.

■ AUTHOR INFORMATION

Corresponding Author

*E-mail: berend-smit@berkeley.edu.

Author Contributions

‖L.J. and J.A.S. contributed equally to this work

Notes

The authors declare no competing financial interest.

■ ACKNOWLEDGMENTS

This work was supported as part of the Center for Gas Separations Relevant to Clean Energy Technologies, an Energy Frontier Research Center funded by the U.S. Department of Energy, Office of Science, Office of Basic Energy Sciences under Award Number DE-SC0001015.

L.J. is a Ph.D. fellow funded by the Foundation of Scientific Research-Flanders (FWO) and is a 2013–2014 grantee of the Commission for Educational Exchange between the United States and Belgium, which administers the Fulbright Belgium and Fulbright Schuman programs. This publication has been made possible by a mobility grant of the Ghent University Special Research Fund. Figure 1 was made with VMD software support. VMD is developed with NIH support by the Theoretical and Computational Biophysics group at the Beckman Institute, University of Illinois at Urbana–Champaign.

■ REFERENCES

(1) Pacala, S.; Socolow, R. Stabilization Wedges: Solving the Climate Problem for the Next 50 Years with Current Technologies. *Science* **2004**, *305*, 968–972.

(2) *The Power to Reduce CO_2 Emissions: The Full Portfolio: 2009 Technical Report*; Technical Report 1020389, Electric Power Research Institute: Palo Alto, CA, 2009.

(3) *Annual Energy Outlook 2011*; Technical Report DOE/EIA-0383(2011), Energy Information Administration, U.S. DOE: Washington, DC, 2011.

(4) Bhown, A. S.; Freeman, B. C. Analysis and Status of Post-Combustion Carbon Dioxide Capture Technologies. *Environ. Sci. Technol.* **2011**, *45*, 8624–8632.

(5) *DOE/NETL Carbon Dioxide Capture and Storage RD&D Roadmap*; Technical Report, National Energy Technology Laboratory: Pittsburgh, PA, 2010.

(6) Mérel, J.; Clausse, M.; Meunier, F. Carbon Dioxide Capture by Indirect Thermal Swing Adsorption Using 13X Zeolite. *Environ. Prog.* **2006**, *25*, 327–333.

(7) Ko, D.; Siriwardane, R.; Biegler, L. T. Optimization of a Pressure-Swing Adsorption ProcessUsing Zeolite 13X for CO_2 Sequestration. *Ind. Eng. Chem. Res.* **2003**, *42*, 339–348.

(8) Chue, K. T.; Kim, J. N.; Yoo, Y. J.; Cho, S. H.; Yang, R. T. Comparison of Activated Carbon and Zeolite 13X for CO_2 Recovery from Flue Gas by Pressure Swing Adsorption. *Ind. Eng. Chem. Res.* **1995**, *34*, 591–598.

(9) Bae, T.-H.; Hudson, M. R.; Mason, J. A.; Queen, W. L.; Dutton, J. J.; Sumida, K.; Micklash, K. J.; Kaye, S. S.; Brown, C. M.; Long, J. R. Evaluation of Cation-Exchanged ZeoliteAdsorbents for Post-Combustion Carbon Dioxide Capture. *Energy Environ. Sci.* **2013**, *6*, 128–138.

(10) D'Alessandro, D. M.; Smit, B.; Long, J. R. Carbon Dioxide Capture: Prospects for New Materials. *Angew. Chem., Int. Ed.* **2010**, *49*, 6058–6082.

(11) Li, J.-R.; Sculley, J.; Zhou, H.-C. Metal-Organic Frameworks for Separations. *Chem. Rev.* **2012**, *112*, 869–932.

(12) *Cost and Performance Baseline for Fossil Energy Plants, Vol. 1: Bituminous Coal and Natural Gas to Electricity*; National Energy Technology Laboratory: Pittsburgh, PA, 2010.

(13) Jänchen, J.; Ackermann, D.; Stach, H.; Brösicke, W. Studies of the Water Adsorption on Zeolites and Modified Mesoporous Materials for Seasonal Storage of Solar Heat. *Solar Energy* **2004**, *76*, 339–344.

(14) Hou, Y.; Vidu, R.; Stroeve, P. Solar Energy Storage Methods. *Ind. Eng. Chem. Res.* **2011**, *50*, 8954–8964.

(15) Wang, Y.; LeVan, M. D. Adsorption Equilibrium of Carbon Dioxide and Water Vapor on Zeolites 5A and 13X and Silica Gel: Pure Components. *J. Chem. Eng. Data* **2009**, *54*, 2839–2844.

(16) Wang, Y.; LeVan, M. D. Adsorption Equilibrium of Binary Mixtures of Carbon Dioxide and Water Vapor on Zeolites 5A and 13X. *J. Chem. Eng. Data* **2010**, *55*, 3189−3195.
(17) Brandani, F.; Ruthven, D. M. The Effect of Water on the Adsorption of CO_2 and C_3H_8 on Type X Zeolites. *Ind. Eng. Chem. Res.* **2004**, *43*, 8339−8344.
(18) Ferreira, D.; Magalhães, R.; Taveira, P.; Mendes, A. Effective Adsorption Equilibrium Isotherms and Breakthroughs of Water Vapor and Carbon Dioxide on Different Adsorbents. *Ind. Eng. Chem. Res.* **2011**, *50*, 10201−10210.
(19) Lee, K.-M.; Lim, Y.-H.; Jo, Y.-M. Evaluation of Moisture Effect on Low-Level CO_2 Adsorption by Ion-Exchanged Zeolite. *Environ. Technol.* **2012**, *33*, 77−84.
(20) Castillo, J.; Dubbeldam, D.; Vlugt, T.; Smit, B.; Calero, S. Evaluation of various water models for simulation of adsorption in hydrophobic zeolites. *Mol. Simul.* **2009**, *35*, 1067−1076.
(21) Di Lella, A.; Desbiens, N.; Boutin, A.; Demachy, I.; Ungerer, P.; Bellat, J.-P.; Fuchs, A. H. Molecular Simulation Studies of Water Physisorption in Zeolites. *Phys. Chem. Chem. Phys.* **2006**, *8*, 5396−5406.
(22) Lee, S. H.; Moon, G. K.; Choi, S. G.; Kim, H. S. Molecular Dynamics Simulation Studies of Zeolite-A: 3. Structure and Dynamics of Na Ions and Water Molecules in a Rigid Zeolite-A. *J. Phys. Chem.* **1994**, *98*, 1561−1569.
(23) Faux, D. A.; Smith, W.; Forester, T. R. Molecular Dynamics Studies of Hydrated and Dehydrated Na-Zeolite-4A. *J. Phys. Chem. B* **1997**, *101*, 1762−1768.
(24) Beauvais, C.; Boutin, A.; Fuchs, A. H. Adsorption of Water in Zeolite Sodium-Faujasite: a Molecular Simulation Study. *C. R. Chim.* **2005**, *8*, 485−490.
(25) Bellat, J.-P.; Paulin, C.; Jeffroy, M.; Boutin, A.; Paillaud, J.-L.; Patarin, J.; Di Lella, A.; Fuchs, A. Unusual Hysteresis Loop in the Adsorption-Desorption of Water in NaY Zeolite at Very Low Pressure. *J. Phys. Chem. C* **2009**, *113*, 8287−8295.
(26) Boddenberg, B.; Rakhmatkariev, G. U.; Hufnagel, S.; Salimov, Z. A Calorimetric and Statistical Mechanics Study of Water Adsorption in Zeolite NaY. *Phys. Chem. Chem. Phys.* **2002**, *4*, 4172−4180.
(27) Hutson, N. D.; Zajic, S. C.; Yang, R. T. Influence of Residual Water on the Adsorption of Atmospheric Gases in Li-X Zeolite: Experiment and Simulation. *Ind. Eng. Chem. Res.* **2000**, *39*, 1775−1780.
(28) Frenkel, D.; Smit, B. *Understanding Molecular Simulation: From Algorithms to Applications*, 2nd ed.; Academic Press: San Diego, 2002.
(29) Olson, D. H. Reinvestigation of the Crystal Structure of the Zeolite Hydrated NaX. *J. Phys. Chem.* **1970**, *74*, 2758−2764.
(30) García-Pérez, E.; Parra, J.; Ania, C.; García-Sánchez, A.; van Baten, J.; Krishna, R.; Dubbeldam, D.; Calero, S. A Computational Study of CO_2, N_2, and CH_4 Adsorption in Zeolites. *Adsorption* **2007**, *13*, 469−476.
(31) Vlugt, T. J. H.; Schenk, M. Influence of Framework Flexibility on the Adsorption Properties of Hydrocarbons in the Zeolite Silicalite. *J. Phys. Chem. B* **2002**, *106*, 12757−12763.
(32) García-Sánchez, A.; Ania, C. O.; Parra, J. B.; Dubbeldam, D.; Vlugt, T. J. H.; Krishna, R.; Calero, S. Transferable Force Field for Carbon Dioxide Adsorption in Zeolites. *J. Phys. Chem. C* **2009**, *113*, 8814−8820.
(33) Berendsen, H. J. C.; Grigera, J. R.; Straatsma, T. P. The Missing Term in Effective Pair Potentials. *J. Phys. Chem.* **1987**, *91*, 6269−6271.
(34) NIST Chemistry WebBook. 2012; http://webbook.nist.gov.
(35) Mähler, J.; Persson, I. A Study of the Hydration of the Alkali Metal Ions in Aqueous Solution. *Inorg. Chem.* **2012**, *51*, 425−438.
(36) Maurin, G.; Bell, R. G.; Devautour, S.; Henn, F.; Giuntini, J. C. Modeling the Effect of Hydration in Zeolite Na+ Mordenite. *J. Phys. Chem. B* **2004**, *108*, 3739−3745.
(37) Maurin, G.; Plant, D. F.; Henn, F.; Bell, R. G. Cation Migration upon Adsorption of Methanol in NaY and NaX Faujasite Systems: A Molecular Dynamics Approach. *J. Phys. Chem. B* **2006**, *110*, 18447−18454.
(38) Plant, D. F.; Maurin, G.; Jobic, H.; Llewellyn, P. L. Molecular Dynamics Simulation of the Cation Motion upon Adsorption of CO_2 in Faujasite Zeolite Systems. *J. Phys. Chem. B* **2006**, *110*, 14372−14378.
(39) Wang, Y.; LeVan, M. D. Adsorption Equilibrium of Binary Mixtures of Carbon Dioxide and Water Vapor on Zeolites 5A and 13X. *J. Chem. Eng. Data* **2010**, *55*, 3189−3195.